# Diverse Heterocyclic Scaffolds as Allosteric Inhibitors of AKT

Jason G. Kettle,* Simon Brown, Claire Crafter, Barry R. Davies, Phillippa Dudley, Gary Fairley, Paul Faulder, Shaun Fillery, Hannah Greenwood, Janet Hawkins, Michael James, Keith Johnson, Clare D. Lane, Martin Pass, Jennifer H. Pink, Helen Plant, and Sabina C. Cosulich

Oncology iMED, AstraZeneca, Alderley Park, Macclesfield, SK10 4TG, United Kingdom

Ⓢ Supporting Information
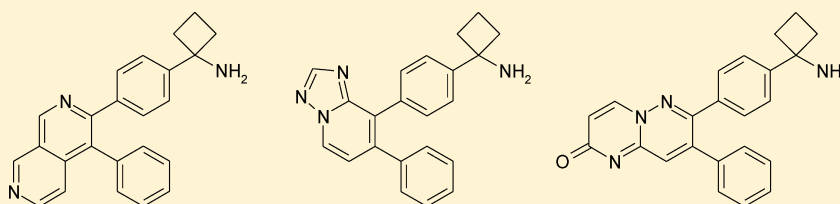
ABSTRACT: Wide-ranging exploration of potential replacements for a quinoline-based inhibitor of activation of AKT kinase led to number of alternative, novel scaffolds with potentially improved potency and physicochemical properties. Examples showed predictable DMPK properties, and one such compound demonstrated pharmacodynamic knockdown of phosphorylation of AKT and downstream biomarkers in vivo and inhibition of tumor growth in a breast cancer xenograft model.

INTRODUCTION

The PI3K-AKT signaling pathway is frequently activated in human cancers and plays a critical role in cell growth, proliferation, motility, and survival.[1] This pathway is activated by several mechanisms in different cancer types, including somatic mutation, deletion, and amplification of genes encoding key components. Because of its prominent role in many cancer types, the PI3K-AKT pathway has become the focus of many cancer therapies, with a number of compounds currently in early clinical trials.[2] Despite the significant efforts invested in the generation of inhibitors of components of this pathway, it remains unclear which cancers will benefit from such therapeutic approaches. The serine threonine kinase AKT (also known as protein kinase B or PKB) is a key effector of the PI3K-AKT signaling pathway and plays a pivotal role in cell survival and proliferation through modulation of a large number of downstream substrates.[3] Following growth factor stimulation of PI3K, AKT is recruited to the plasma membrane. Colocalization with PDK1 at the plasma membrane allows the phosphorylation of threonine 308 (Thr308), located in the AKT activation loop. This phosphorylation event is necessary and sufficient for AKT activation.[4] Further phosphorylation of AKT on serine 473 (Ser473), located in the C-terminal hydrophobic motif by the mTOR complex 2,[5] allows for maximal activation of the AKT enzyme.

There are three mammalian isoforms of AKT (AKT1, -2, and -3) that are broadly expressed in most normal tissues and are also expressed in most tumor types to varying degrees. The three enzymes have a similar organizational structure: an N-terminal PH domain, a central serine/threonine catalytic domain, and a short regulatory region at the C-terminal, also called the hydrophobic motif.[6] On the basis of the strong rationale for targeting AKT in cancer, many efforts have been made to identify AKT inhibitors with acceptable pharmaceutical properties. However, because of the high sequence identity between the different AKT isoforms and other AGC kinases, the development of AKT-specific and isoform-specific inhibitors has been a real challenge for the pharmaceutical industry. The most common approaches described to date have been either through the design of compounds that are ATP-competitive or prevent the formation of the active enzyme.[7] Inhibitors targeting the PH domain have also been described.[8] AKT inhibitors that are ATP competitive paradoxically cause the hyperphosphorylation of AKT at its two main regulatory sites (Thr308 and Ser473) as a consequence of a disrupted feedback mechanism caused by the direct binding of the inhibitor to the kinase.[9] In contrast, allosteric inhibitors cause a decrease in the phosphorylation of AKT at these two sites. The clinical significance of these findings is still unclear, with a number of AKT inhibitors currently being tested in clinical trials. These include allosteric inhibitors of inactive AKT, such as MK-2206 (**1**),[10] and ATP-competitive inhibitors of active enzyme, such as GDC0068 (**2**),[11] GSK2141795,[12] and AZD5363 (Figure 1).[13] It will be important to establish whether the different modes of inhibition of AKT will deliver efficacy in late-stage clinical trials. In order to compliment our own work with AZD5363, we were interested in exploring additional opportunities around an allosteric inhibitor of inactive AKT profile such as that described for **1**.

RESULTS AND DISCUSSION

Design of Inhibitors. At the outset of this work, since the binding mode of **1** had not yet been reported, it was unclear
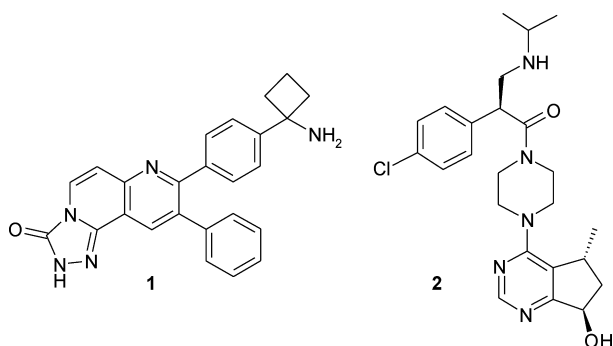
Figure 1. Allosteric inhibitor of inactive AKT, MK-2206 (**1**), and an example of an inhibitor of active AKT, GDC-0068 (**2**).

which elements of the structure were critical for binding to AKT. Analysis of the extensive literature[14] of this series did however give an indication of which groups had been successfully varied and those which had largely been held constant, which was suggestive of an absolute basic pharmacophore. Figure 2 illustrates assumptions about the general requirements for binding based on published literature, together with our proposed strategy for optimization based on exploration of scaffolds outside of the perceived basic pharmacophore. The central scaffolds in the published SAR (Figure 2, left panel), often groups such as pyridine or quinoline, always retain an sp[2] nitrogen atom, which suggested a potential role in hydrogen bonding to AKT. Subsequent to this work, the first reported crystal structure of a compound related to **1** bound to AKT has been disclosed.[15] While this structure confirms binding of inhibitor to the PH domain and C- and N-terminal lobes of the inactive kinase, no such hydrogen bond is observed, however. The scaffold itself can be extended in a number of ways, with examples of mono-, bi-, and tricyclic ring systems all reported. The lower pendant phenyl ring in all iterations remains unsubstituted, suggesting a relatively small lipophilic pocket in this region, and indeed, the related crystal structure shows this to be the case. A basic benzylic amine functionality appended to the upper phenyl ring is a common feature, although examples indicate that a wide variety of cyclic amines are tolerated, including those with relatively large overall size. The later reported structure indicated that this basic group is involved in a critical water-mediated hydrogen bond to asparagine 54 (Asn54) on the PH domain. The proposed strategy to investigate alternative core structures that would, it was hoped, provide novel scaffolds able to potently inhibit AKT can be broken down into several

related themes. First, we wished to explore linear structures in which one ring junction contained a bridgehead nitrogen atom (Figure 2, right panel). Such a strategy has previously been successful in generating alternative scaffolds of quinazoline for inhibition of a variety of protein kinases,[16] and indeed, independent of this work, a group at Bayer has recently reported success with this strategy against AKT.[17] In addition, we wished to explore opportunities for alternatively fused rings, here termed ring fusion "south" or "north", dependent on the direction of the scaffold. Such changes have not been described previously, and it should be noted that for ring fusion north such an approach necessarily removes what we (at the time) perceived to be a critical sp[2] nitrogen atom. Nevertheless, it was felt that introduction of nitrogen into the resulting five-membered ring might be able to compensate for this loss, if some flexibility in nitrogen lone pair orientation might be tolerated. Finally, we explored a small number of additional novel scaffolds that were shown to be both synthetically accessible and novel, with energy-minimized conformations of all ideas proposed overlaid with those of the working pharmacophore to ensure consistency.

Compound **1** represents a highly optimized candidate drug. In order to be able to benchmark the utility of any novel scaffolds synthesized, it was important to use a suitable reference compound of similar size rather than **1** itself. The primary goal was to understand which, if any, novel scaffold could offer a platform for AKT inhibition, with further optimization of any scaffold reserved for subsequent studies. In the event, we selected compound **3** (Table 1) to act as the reference since quinoline is the simplest of the literature-validated bicyclic scaffolds. Although compound **3** has not previously been reported, the quinoline core has been described with a variety of alternative, extended amines in place of the cyclobutylamine moiety present in **1**.[18] Reference compound **3** is able to potently inhibit phosphorylation of AKT in cells at both Thr308 and Ser473, consistent with its mechanism of action, with IC_{50}'s of 0.557 and 0.250 μM, respectively (Table 1). Enzyme activity was routinely assayed for all analogues synthesized. It should be noted, however, that the enzymatic assay utilized here was one using active enzyme, designed specifically for the purpose of testing inhibitors of catalysis, rather than, compounds that bind to and stabilize inactive enzyme. Nevertheless, such an assay is able to pick up activity via both modes of inhibition—the quoted activity is therefore an underestimate of the true level of potency—and generally cell activity was used to monitor chemistry progress. Compound **3** demonstrates a moderately high lipophilicity
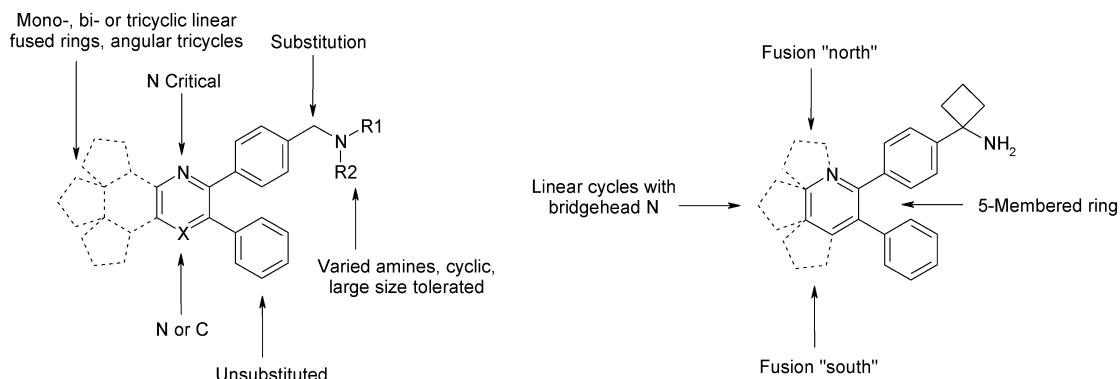

Figure 2. SAR for allosteric inhibition of AKT based on published data (left panel) and strategy for optimization to give novel cores (right panel).

Table 1. Bicyclic Scaffolds with Bridgehead Nitrogen—Activity and Selected Physicochemical Data

	Structure[1]	AKT1 IC$_{50}$	Cell p-AKT T308 IC$_{50}$[2]	Cell p-AKT S473 IC$_{50}$[3]	LogD	Rat PPB % free[4]	Solubility (µM)[5]
3		0.243	0.557	0.250	3.6	1.1	290
4		0.926	2.428	1.232	3.3		27
5		0.528	0.391	0.216	12.3		
6		0.199	0.205	0.151	3.2		150
7		0.387	0.182	0.124	2.8	6.8	1900
8		0.348	0.082	0.092	2.0		110
9		8.665	1.615	2.170	0.2		1900

[1]R1 = 4-phenylcyclobutyl-1-amine, R2 = Ph. [2]Inhibition of phosphorylation of Thr308 on AKT in BT474 cells. [3]Inhibition of phosphorylation of Ser473 on AKT in MDAMB468 cells. [4]Plasma protein binding in rat (Han Wistar). [5]Aqueous solubility measured at pH 7.4. All IC$_{50}$ data is reported as micromolar and is the mean of at least n = 2 data points, and each has a SEM ± 0.2 log units.

Scheme 1. Synthesis of Reference Compound 3 and Imidazopyridazine Scaffold 5
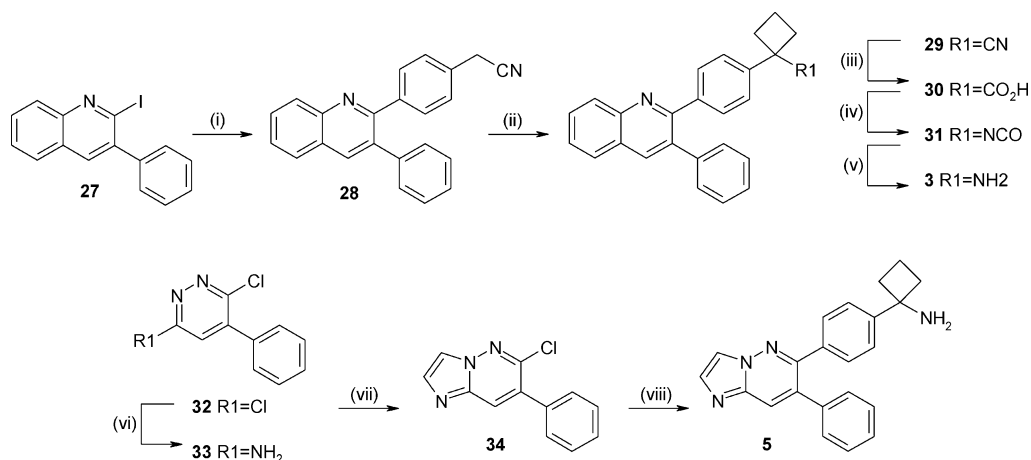
Reagents and conditions: (i) 2-[4-(4,4,5,5-tetramethyl-1,3,2-dioxaborolan-2-yl)phenyl]acetonitrile, Pd(PPh$_3$)$_4$, K$_2$CO$_3$, dioxane, 100 °C, 18 h; (ii) tetra-n-butylammonium bromide, 1,3-dibromopropane, toluene, water, 100 °C, 1 h; (iii) KOH, 2,2′-oxidiethanol, 245 °C, 75 min; (iv) DPPA, Et$_3$N, dichloromethane, 25 °C, 4 h; (v) aq HCl, 60 °C, 5.5 h; (vi) NH$_3$, ethanol, 150 °C, 24 h; (vii) 2-chloroacetaldehyde, H$_2$O, 60 °C, 16 h; (viii) tert-butyl N-[1-[4-(4,4,5,5-tetramethyl-1,3,2-dioxaborolan-2-yl)phenyl]cyclobutyl]carbamate, Pd(PPh$_3$)$_4$, Zn(OAc)$_2$, Na$_2$CO$_3$, 1,4-dioxane, 100 °C, 1 h, then TFA, dichloromethane, rt, 1 h.

(log D = 3.6), and consequently low free drug (1.1% free drug measured in Han Wistar rat plasma) and a modest solubility of 290 µM.

Synthesis of AKT Inhibitors. Herein is discussed the synthesis of representative structures explored during the course of this work as detailed in Table 4. Complete experimental details of all compounds described can additionally be found in the Supporting Information. Reference quinoline 3 was synthesized from iodoquinoline starting material 27 via a sequence of Suzuki coupling to give phenylacetontrile 28, followed by installation of the cyclobutyl moiety through double alkylation with dibromopropane (Scheme 1). The requisite amine was obtained following

Curtius rearrangement of acid 30, and hydrolysis of the relatively stable resulting isocyanate 31, to give 3. Starting with commercially available dichloropyridazine 32, amination gave intermediate 33, which was used in the synthesis of imidazopyridazine 5. Reaction of 33 with chloroacetaldehyde gave bicycle 34, which yielded target 5 following Suzuki coupling and deprotection to install the requisite cyclobutyl-amine side chain.

Pyrazolopyridine 39 was synthesized via a [3 + 2] cyclo-addition between 1-aminopyridinium iodide and acetylenic ester 38 (Scheme 2), itself assembled in a short sequence from bromide 35 involving acetylenic coupling and double alkylation with ethyl chloroformate. Target scaffold 6 was subsequently

Scheme 2. Synthesis of 6,5-Bridgehead-Based Scaffolds 6 and 7
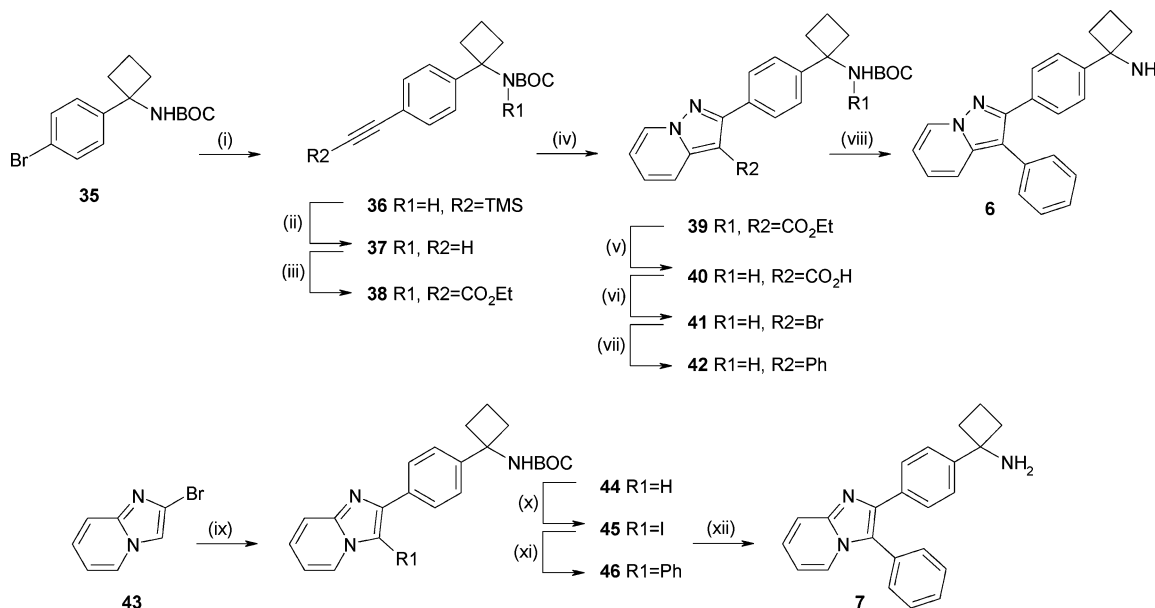
Reagents and conditions: (i) TMS–acetylene, Pd(PPh$_3$)$_2$Cl$_2$, CuI, Et$_3$N, tetrahydrofuran, 70 °C, 12 h; (ii) K$_2$CO$_3$, methanol, rt, 1 h; (iii) LDA, tetrahydrofuran, ClCO$_2$Et, −78 °C to rt, 1.5 h; (iv) 1-aminopyridinium iodide, DBU, CH$_3$CN, 0 °C to rt, 18 h; (v) NaOH, ethanol, 100 °C, 2 h; (vi) NBS, Na$_2$CO$_3$, dimethylformamide, rt, 1 h; (vii) phenylboronic acid, aq Na$_2$CO$_3$, Pd(PPh$_3$)$_2$Cl$_2$, dimethylformamide, 1,2-dimethoxyethane, ethanol, H$_2$O, 150 °C, 15 min; (viii) TFA, dichloromethane, rt, 2 h; (ix) *tert*-butyl *N*-[1-[4-(4,4,5,5-tetramethyl-1,3,2-dioxaborolan-2-yl)phenyl]cyclobutyl]-carbamate, aq Na$_2$CO$_3$, Pd(PPh$_3$)$_2$Cl$_2$, dimethylformamide, 1,2-dimethoxyethane, ethanol, H$_2$O, 150 °C, 10 min; (x) NIS, CH$_3$CN, rt, 1 h; (xi) phenylboronic acid, aq Na$_2$CO$_3$, Pd(PPh$_3$)$_2$Cl$_2$, dimethylformamide, 1,2-dimethoxyethane, ethanol, H$_2$O, 150 °C, 15 min; (xii) TFA, dichloromethane, rt, 2 h.

Scheme 3. Synthesis of Imidazopyrazine Scaffold 11
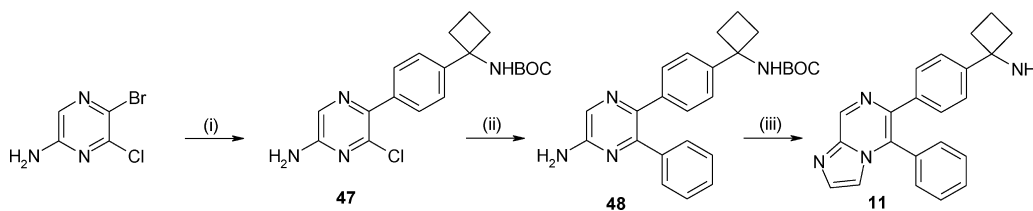
Reagents and conditions: (i) *tert*-butyl *N*-[1-[4-(4,4,5,5-tetramethyl-1,3,2-dioxaborolan-2-yl)phenyl]cyclobutyl]carbamate, Pd(PPh$_3$)$_4$, aq Na$_2$CO$_3$, 100 °C, 2 h; (ii) phenylboronic acid, Pd(PPh$_3$)$_4$, aq Na$_2$CO$_3$, dioxane, 110 °C, 1 h; (iii) 2-chloroacetaldehyde, H$_2$O, dimethylformamide, 70 °C, 1.5 h then HCl, dioxane, dichloromethane, rt, 1 h.

obtained in a sequence involving ester hydrolysis, decarboxylative bromination to give **41**, followed by Suzuki coupling and deprotection. Its regioisomer **7** was obtained more simply from imidazopyridine **43** through a Suzuki–iodination–Suzuki coupling protocol to give **46** and then **7** via deprotection. 5-Bromo-6-chloropyrazin-2-amine served as starting material for synthesis of the imidazopyrazine core **11** (Scheme 3). Judicious selection of boronic acid coupling partners allowed selective differentiation of first the bromo and then chloro functionalities to yield aminopyrazine **48**. Treatment with chloroacetaldehyde to form the imidazole ring and then deprotection afforded **11**.

Fused south naphthyridine analogue **15** was obtained using a procedure described by Wu.[19] Phenylacetylene **37** was coupled with an *o*-bromopyridine aldehyde to give **49**. The oxime product **50** formed by condensation with *O*-methylhydroxylamine was cyclized under copper catalysis conditions to give naphthyridine **51**. From here, Suzuki coupling to install the pendant phenyl ring and deprotection afforded the target **15** (Scheme 4). Finally, pyridine scaffold **26** was synthesized by sequential selective Suzuki coupling on 5,6-dichloropyridine-3-

carbonitrile (Scheme 5). Deprotection under acidic conditions resulted in concomitant hydrolysis of the nitrile group to primary amide **26**.

Structure–Activity and Structure–Property Relationships for Scaffolds with Bridgehead Nitrogen. Table 1 shows enzyme and cell activity data together with measured log *D*, rat plasma protein binding, and aqueous solubility for the reference compound **3** together with a variety of alternative scaffolds that all feature a single bridgehead nitrogen atom. To incorporate this feature necessitates a switch to a 5,6-ring system (**4**, **5**), a 6,5-ring system (**6–8**), or, where the 6,6-ring is maintained as in **9**, incorporation of an exocyclic carbonyl group to maintain valence. All of these analogues maintain an sp^2 nitrogen at a position equivalent to that found in quinoline **3**. Compound **4** shows a drop in potency across all assays relative to the quinoline, and solubility is lower despite a similar log *D*. Interestingly, incorporation of an extra nitrogen in the five-membered ring, as in **5**, results in an increase in potency to give a profile close to that of the quinoline, albeit with much improved free drug (over 10-fold). Initially more speculative

Scheme 4. Synthesis of Fused South Analogue 15
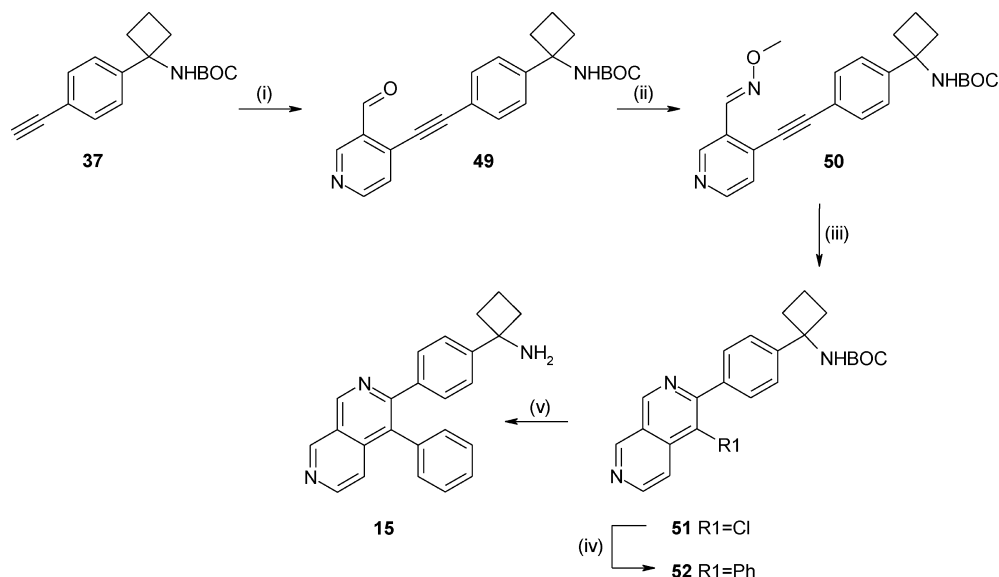
Reagents and conditions: (i) 4-bromopyridine-3-carbaldehyde, Pd(PPh₃)₄, CuI, Et₃N, CH₃CN, rt, 42 h; (ii) MeONH₂.HCl, Et₃N, dichloromethane, rt, 5.5 h; (iii) CuCl₂, DMA, 100 °C, 3.5 h; (iv) phenylboronic acid, Pd(OAc)₂, potassium orthophosphate, toluene, 80 °C, 2 h; (v) HCl, dioxane, dichloromethane, rt, 15 min.

Scheme 5. Synthesis of Pyridine Scaffold 26
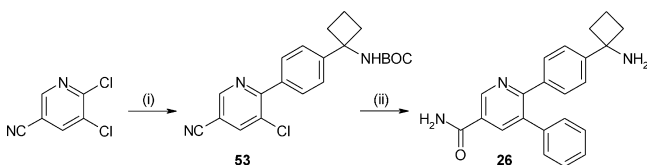
Reagents and conditions: (i) *tert*-butyl *N*-[1-[4-(4,4,5,5-tetramethyl-1,3,2-dioxaborolan-2-yl)phenyl]cyclobutyl]carbamate, 1,1-bis(di-*tert*-butylphosphino)ferrocene palladium dichloride, aq K₂CO₃, CH₃CN, 80 °C, 18 h; (ii) phenylboronic acid, Pd(OAc)₂, potassium orthophosphate, toluene, 80 °C, 2 h then HCl, dioxane, dichloromethane, methanol, rt, 3.5 h.

analogues such as **6** and **7**, in which the central six-membered-ring scaffold common to all existing disclosures is swapped for a five-membered ring, also show potent inhibition. Pyrazolopyridine **6** and imidazopyridine **7** show an activity similar to that of quinoline **3**, with the latter showing reduced lipophilicity and significantly improved free drug and solubility. An analogue of **7** with a primary carboxamide appended, **8** was synthesized since overlays with **1** indicated this vector overlays with the triazolone moiety. This modification resulted in improved potency with the IC₅₀ reaching sub-100 nM in cells, together with a significant drop in lipophilicity, although solubility remains modest. Pyridazinopyrimidinone **9** represents an interesting alternative core to quinoline **3**, showing a dramatically lowered log *D* and high solubility. In this case, however, potency in cells is substantially impacted; while it may be tempting to speculate a permeability issue due to low log *D*, the reduced activity in the enzyme assay suggests an inherent mismatch in binding at the target level.
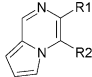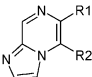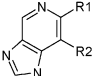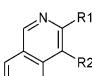
Structure−Activity and Structure−Property Relationships for Scaffolds with a Fused South Ring Structure. We next examined the effect of fusing a second ring to the lower part of the scaffold, a modification not reported in the literature. Initially, a series of 5,6-fused ring systems exemplified

by **10−12** were synthesized (Table 2). Compound **10** and its aza-homologue **11** showed similar, if slightly reduced, activity to reference **3**, with a significant reduction in log *D* contributing to very high solubility and free drug levels in the case of **11**. Both of these analogues again exhibit a bridgehead nitrogen. Compound **12**, without this feature shows reduced activity, possibly due to the bulky nitrogen substituent causing unfavorable twists in the adjacent pendant aromatic groups. Moving on to examine 6,6-ring systems, compound **13** is the exact analogue of reference **3**, albeit now with an isoquinoline scaffold in place of quinoline. In this case, the potency and physicochemical property profile is indistinguishable from reference **3**. The effect of successive aza-substitution was examined in the four naphthyridine isomers **14−17**. Interestingly, each of these showed an improved potency over the corresponding isoquinoline/quinoline core. Aza substitution imparts over 1.5 log units lowered lipophilicity in each case, and this manifests in much improved solubility and good free drug levels. 1,7- And 2,7-napthyridines (**14** and **15**, respectively) appear preferred over 2,6- and 1,6-naphthyridines (**16** and **17**, respectively).
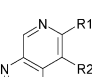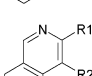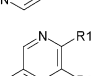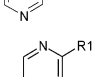
Structure−Activity and Structure−Property Relationships for Scaffolds with a Fused North Ring Structure. Literature exemplification of allosteric AKT inhibitors allude to the importance of the quinoline (or similar) ring nitrogen. Extending this work to look at ring fusion in the direction of this atom carried the risk then that activity may be significantly impacted. We speculated that incorporation of additional ring heteroatoms might be able to compensate for loss of the quinoline nitrogen. Gratifyingly, pyrazolopyridine **18** and imidazopyridine **19** both proved to be active, with the latter having a similar activity profile to quinoline **3**, with the additional benefit of a substantially lowered log *D*, albeit with similar solubility levels (Table 3). Compound **20**, which does not contain a ring nitrogen atom in the vicinity of its position in quinoline **3**, shows reduced activity as anticipated. Triazolopyridine scaffold **21** represents a potent alternative to quinoline,

Table 2. Ring-Fused Scaffolds (South)—Activity and Selected Physicochemical Data

	Structure[1]	AKT1 IC$_{50}$	Cell p-AKT T308 IC$_{50}$[2]	Cell p-AKT S473 IC$_{50}$[3]	LogD	Rat PPB % free[4]	Solubility (μM)[5]
10		0.787	0.604	0.483	2.5		1500
11		1.262	0.386	0.365	1.3	37.1	2500
12		8.976	1.203	1.535	2.0		
13		0.301	0.535	0.179	3.6		470
14		0.188	0.089	0.047	2.0		1500
15		0.117	0.048	0.037	2.2	13.0	2200
16		0.193	0.054	0.098	2.2	10.5	1400
17		0.465	0.167	0.104	1.7		2000

[1]R1 = 4-phenylcyclobutyl-1-amine, R2 = Ph. [2]Inhibition of phosphorylation of Thr308 on AKT in BT474 cells. [3]Inhibition of phosphorylation of Ser473 on AKT in MDAMB468 cells. [4]Plasma protein binding in rat (Han Wistar). [5]Aqueous solubility measured at pH 7.4. All IC$_{50}$ data is reported as micromolar and is the mean of at least $n = 2$ data points, and each has a SEM ± 0.2 log units.

again with a dramatically lowered log D and higher solubility. The alternative triazolopyridine isomer **22** shows slightly reduced potency. Whereas all of these scaffolds contain a bridgehead nitrogen, good potency is also achieved from a simple benzimidazole core **23**. Here, a reduced log D relative to quinoline is combined with a potentially useful additional vector for further optimization in the pendant *N*-methyl substituent. Table 3 also contains additional scaffolds that were examined as part of this work. Quinazolone cores **24** and **25** are interesting, since they allow each of the pendant phenyl rings to be linked to the core via a nitrogen atom, as opposed to carbon in all previous examples. However, despite substantial log D and solubility improvements, both cores show severely compromised potency. As expected, the isomer **24** that retains a quinoline-like nitrogen demonstrates the most activity. The overall reduced potency, even in this case, may be due to unfavorable interaction between the lower carbonyl and pendant phenyl group, although QM calculations indicate minimal difference in the pendant phenyl torsion angle between **24** and quinoline **3**. Pyridine amide derivative **26** was also synthesized. Pyridine, specifically with a pendant nitrile group, has previously been validated as a scaffold for AKT inhibition,[20] although only previously combined with extended lipophilic amine side chains; in this case, even with a much truncated basic side chain, good potency is maintained and is combined with exceptional free drug levels.

Docking Studies. The recently disclosed[15] crystal structure of an analogue of **1** was used as the basis for docking studies of the most potent inhibitor discovered here, compound **15** as shown in Figure 3. A model of **15** was built[21] and then docked[22] into the native crystal structure (PDB code 3O96) using standard precision and no constraints. Satisfyingly, the docked molecule overlaid well with the literature compound (omitted for clarity), and we assume the same bridging water interaction between primary amine, Water 455, and Asn54. Trp80 appears to make a significant π−π stacking interaction with the aza isoquinoline scaffold of **15**, and may in part explain the high potency seen with a seemingly diverse set of heterocyclic scaffolds. The pendant naked phenyl substituent seen in all inhibitors sits in a relatively small lipophilic pocket bounded by Leu210, Leu264, Tyr272, Ile290, and Asp292, and the cyclobutyl ring sits in an adjacent pocket bounded by Tyr272, Asp274, and Gly294. No further optimization was performed.

DMPK and in Vivo Activity of Selected Examples. A selection of analogues that showed a good combination of potency and acceptable lipophilicity/solubility was examined in in vitro and in vivo DMPK assays, specifically rat and human in vitro hepatocyte clearance assays and rat iv and po studies (Table 4). Reference **3** was first benchmarked. This compound showed high rat in vitro clearance, but despite this, moderate in vivo clearance was observed, albeit with no oral exposure.

Table 3. Ring-Fused Scaffolds (North), Quinazoline Scaffolds 24 and 25, and Pyridine Scaffold 26—Activity and Selected Physicochemical Data

	Structure[1]	AKT1 IC$_{50}$	Cell p-AKT T308 IC$_{50}$[2]	Cell p-AKT S473 IC$_{50}$[3]	LogD	Rat PPB % free[4]	Solubility (µM)[5]
18		2.716	1.192	0.824	2.9		170
19		1.807	0.324	0.388	2.0		550
20		5.404	2.182	2.481	1.7		2500
21		2.668	0.479	0.661	1.7		1000
22		2.135	0.369	0.293			
23		2.799	0.343	0.359	2.5		190
24		7.024	2.616	2.082	1.5		2300
25		41.722	5.895	7.730	1.6		1400
26		1.042	0.422	0.322	1.3	41.9	270

[1]R1 = 4-phenylcyclobutyl-1-amine, R2 = Ph. [2]Inhibition of phosphorylation of Thr308 on AKT in BT474 cells. [3]Inhibition of phosphorylation of Ser473 on AKT in MDAMB468 cells. [4]Plasma protein binding in rat (Han Wistar). [5]Aqueous solubility measured at pH 7.4. All IC$_{50}$ data is reported as micromolar and is the mean of at least n = 2 data points, and each has a SEM ± 0.2 log units.
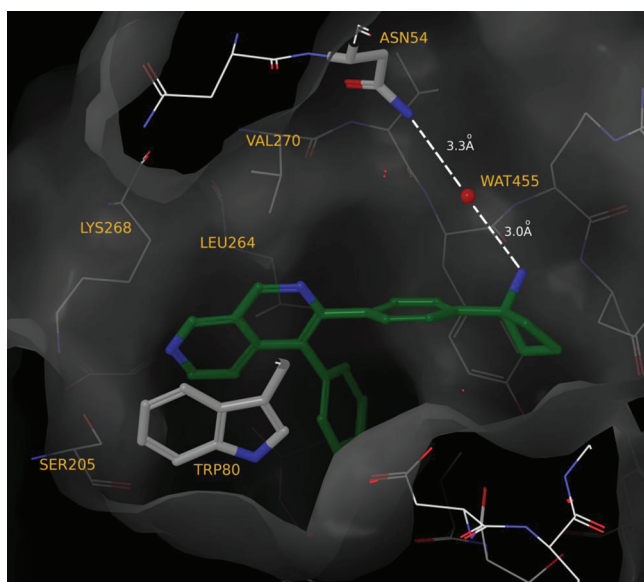

Figure 3. Compound **15** docked into AKT based on PDB code 3O96. Trp80 $\pi-\pi$ stacks with the aza isoquinoline scaffold, and there is an assumed water-mediated hydrogen bond between the inhibitor primary amine and Asn54.

Human in vitro clearance for this reference was significantly lower than in rat. Bridgehead analogues **5** and **6** both exhibited moderate to high clearance and consequently no oral exposure. Interestingly compound **7**, the positional isomer of **6**, shows a bioavailability of 36%, despite a moderately high in vivo clearance. Generally, the in vitro hepatocyte data predicted in vivo clearance within a reasonable spread in rat, where both data points existed. Figure 4 shows the predicted (from hepatocytes) versus measured in vivo clearance for the compounds in Table 4, according to the well-stirred model.[23] In vivo clearance is predicted to within a 2-fold range, a reasonable approximation. Compound **11** shows a similar bioavailability, here combined with low in vitro clearance in both rat and human hepatocytes. Compound **15**, the most potent scaffold identified from this work, shows very high human in vitro clearance although modest rat in vivo clearance. Finally, pyridine analogue **26** shows the lowest clearance in both in vitro and in vivo assays and consequently good bioavailability of 48%. The combination of this compound's good potency and very high free drug levels made it a candidate for further in vivo efficacy profiling.

Biological Activity. The biological activity and specific pharmacology of compound **26** was characterized by measuring the phosphorylation of its downstream substrate PRAS40 in the BT474c breast adenocarcinoma cell line. Compound **26** was

Table 4. Rat[a] and Human in Vitro Metabolism and Rat in Vivo DMPK Properties

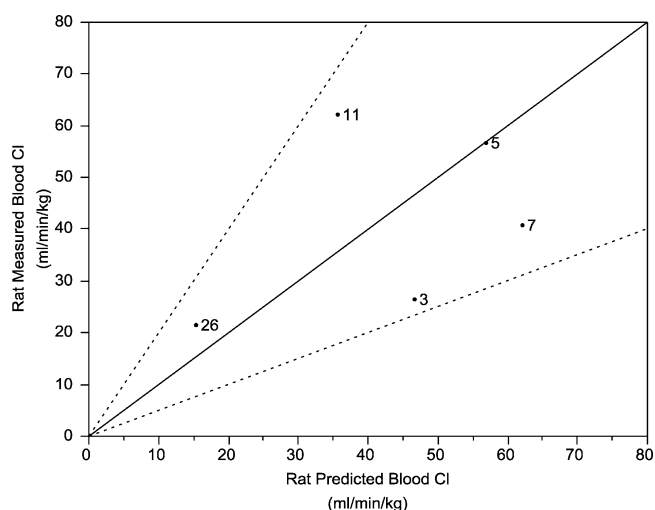|	Cl_{int} (μL/min/10^{-6} cells)		rat iv Cl^b (mL/min/kg)	rat Vdss (l/kg)	rat po bioavailability %
	rat hepatocytes	human hepatocytes			
3	148	14	26	3.1	0
5	274	8	57	2.3	0
6			171	8.0	0
7	291	18	41	10.3	36
11	16	3	62	10.3	30
15		300	40	0.3	
26	4	3	21	11.1	48

[a]Han Wistar. [b]Blood clearance.

Figure 4. Plot of predicted in vivo clearance values versus measured, based on in vitro scaling from rat hepatocyte data for selected compounds. The solid line is a 1:1 correlation and dotted lines represent ±2-fold spread.

shown to potently inhibit the phosphorylation of PRAS40 (Figure 5). Consistent with a prevention of activation mechanism of action, compound **26** also inhibited the phoshorylation of AKT on Ser473 and Thr308. Furthermore, compound **26** inhibited the phosphorylation of ribosomal protein S6, a downstream effector of the PI3K-AKT pathway.

The effects of compound **26** in vivo were characterized by measuring the pharmacodynamic activity of this compound in a BT474c breast adenocarcinoma xenograft model. Following acute doses of 100 and 200 mg/kg, compound **26** potently inhibited the phosphorylation of its downstream substrate GSK3β as well as the phosphorylation of AKT (Ser473), with a potency consistent with its pharmacokinetic profile (Figure 6). The in vivo activity of compound **26** was further characterized by measuring the effects on the growth of tumor cell xenografts. Continuous (daily) oral dosing of compound **26** (100 and 200 mg/kg) to nude mice bearing BT474c breast adenocarcinoma xenografts resulted in inhibition of tumor growth in a dose-dependent manner. When dosed at 200 mg/kg daily, compound **26** caused significant tumor growth inhibition (Figure 7).

Conclusions. Inhibition of the AKT pathway represents a significant current focus for oncology drug discovery, and agents that target both active and inactive AKT are in clinical trials. Both profiles offer potential benefits and risks, and the true value of these individual strategies will emerge in due course. Known quinoline-based inhibitors of inactive AKT have demonstrated a unique cellular phenotype when compared with inhibitors of active kinase, and here we have demonstrated that a broad range of readily accessible alternative scaffold templates also have the potential to provide a platform for AKT inhibition, many with improved potency and physicochemical properties. Subsequent to this work, a range of other scaffolds has also been reported to effectively mimic quinolines in the
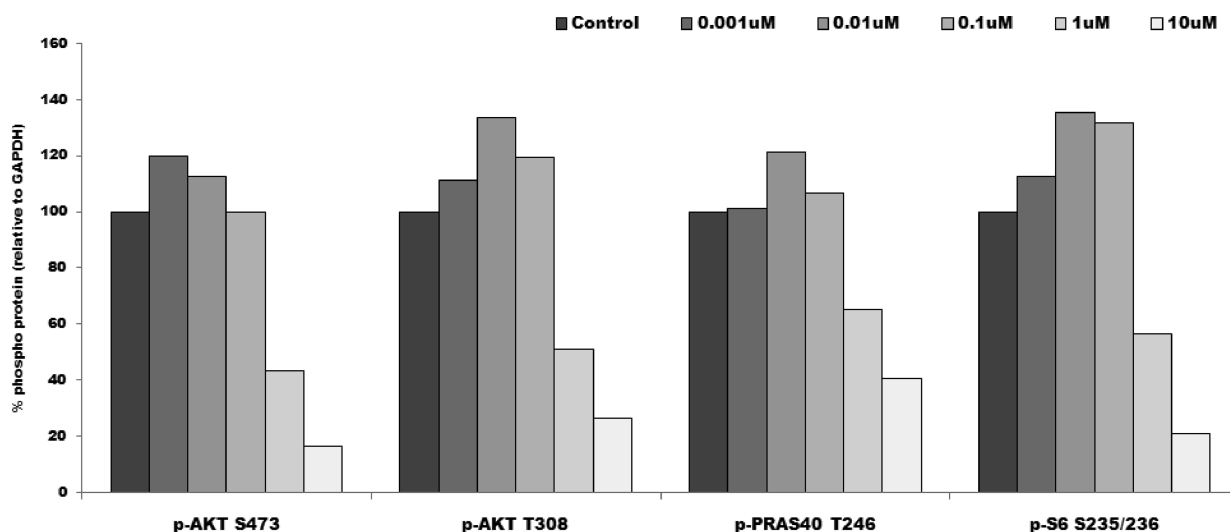

Figure 5. Effects of compound **26** on AKT pathway proteins in the BT474c breast adenocarcinoma cell line at 24 h.
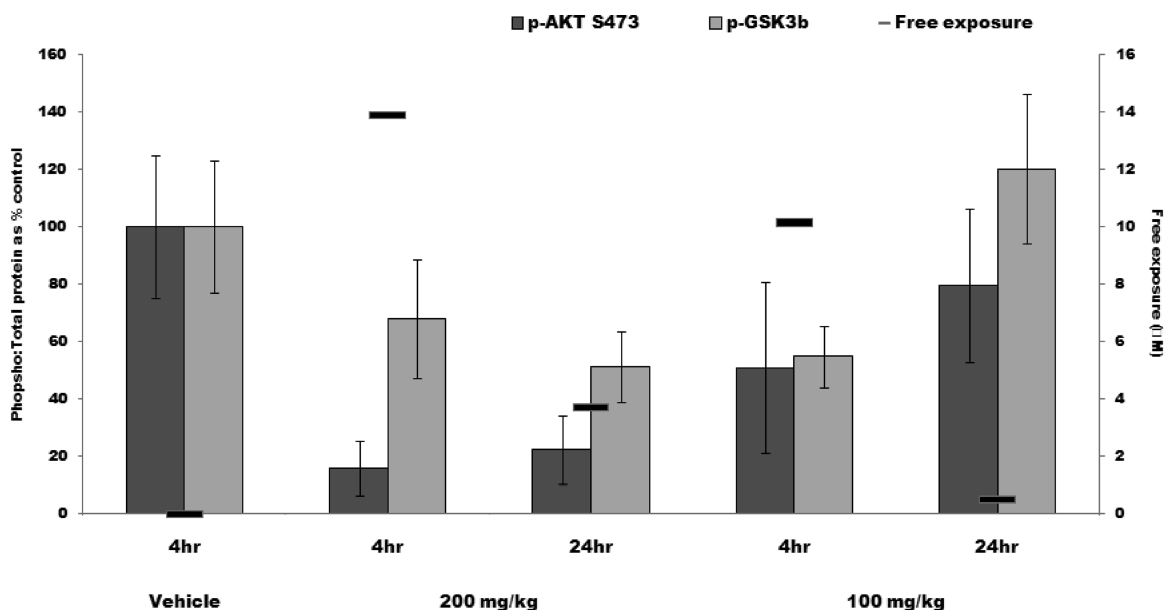
Figure 6. Pharmacodynamic study of compound **26** in nude mice bearing a BT474c xenograft from a single oral dose of 100 and 200 mg/kg at 4 and 24 h time points.
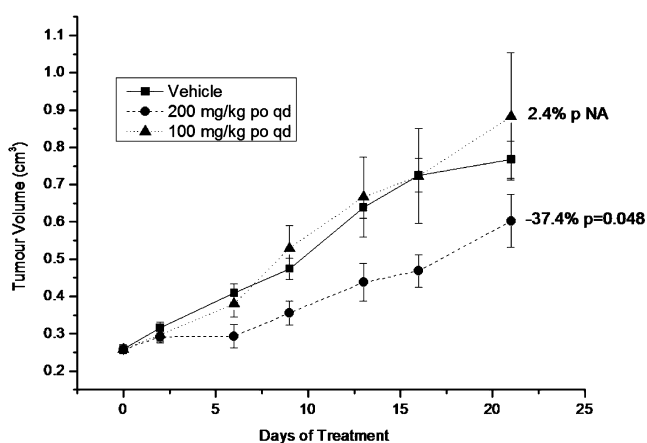

Figure 7. Tumor growth inhibition study of compound **26** in BT474c xenografts growing in nude mice. Compound was dosed once a day orally for 21 days at 100 and 200 mg/kg.

context of AKT inhibition, such as imidazopyridines,[24] furopyridines,[25] and chromenones,[26] further broadening the pharmacophore for activity.

■ EXPERIMENTAL METHODS

Chemistry. All reactions were performed under inert conditions (nitrogen) unless otherwise stated. All solvents and reagents were purchased from commercial sources and used without further purification. For coupling reactions, all solvents were dried and degassed prior to reaction. Reactions performed under microwave irradiation utilized either a Biotage initiator or CEM Discover microwave. Upon workup, organic solvents were typically dried prior to concentration with anhydrous $MgSO_4$ or Na_2SO_4. Flash silica chromatography was typically performed on an Isco Companion, using Silicycle silica gel (230−400 mesh, 40−63 μm cartridges), Grace Resolv silica cartridges, or Isolute Flash Si or Si II cartridges. Reverse-phase chromatography was performed using a Waters XBridge Prep C18 OBD column (5 μm silica, 19 mm diameter, 100 mm length), using decreasingly polar mixtures of either water (containing 1% NH_3) and MeCN, or water (containing 0.1% formic acid) and MeCN as eluents. Analytical LC−MS was performed on a Waters 2790 LC with

a 996 PDA and 2000 amu ZQ single quadrupole mass spectrometer using a Phenomenex Gemini 50 × 2.1 mm, 5 μm, C18 column, or UPLC was performed on an Waters Acquity binary solvent manager with Acquity PDA and an SQD mass spectrometer using a 50 × 2.1 mm, 1.7 μm BEH column from Waters, and purities were measured by UV absorption at 254 nm or TIC and are ≥95% unless otherwise stated. NMR spectra were recorded on a Bruker Av400 or Bruker DRX400 spectrometer at 400 MHz in DMSO-d_6 at 303 K unless otherwise indicated. ^{1}H NMR spectra are reported as chemical shifts in parts per million (ppm) relative to an internal solvent reference.

2-(4-(3-Phenylquinolin-2-yl)phenyl)acetonitrile (28). Pd-$(PPh_3)_4$ (0.21 g, 0.2 mmol) was added to 2-(4-(4,4,5,5-tetramethyl-1,3,2-dioxaborolan-2-yl)phenyl)acetonitrile (0.94 g, 3.9 mmol), **27** (1.22 g, 3.7 mmol), and aq K_2CO_3 (2 M, 5.53 mL, 11.1 mmol) in dioxane (31 mL) and the mixture stirred at 100 °C for 18 h. The reaction mixture was partitioned between ethyl acetate and water; the organic layer was washed with water and then saturated brine, dried, and concentrated; and the crude product was purified by silica chromatography (5−30% ethyl acetate in isohexane) to afford **28** (1.1 g, 93%) as a yellow foam: ^{1}H NMR δ 4.05 (2H, s), 7.25−7.39 (7H, m), 7.39−7.47 (2H, m), 7.61−7.71 (1H, m), 7.82 (1H, ddd), 8.09 (2H, dd), 8.41 (1H, s); m/z (ES+) $(M + H)^+$ = 321.

1-(4-(3-Phenylquinolin-2-yl)phenyl)cyclobutanecarbonitrile (29). Tetra-n-butylammonium bromide (0.025 g, 0.1 mmol), 1,3-dibromopropane (0.17 mL, 1.7 mmol), and **28** (0.5 g, 1.6 mmol) were added to KOH (0.44 g, 7.8 mmol) in toluene (3 mL) and water (0.23 mL) at 70 °C. The resulting mixture was heated at 100 °C for 70 min, cooled to room temperature, and diluted with toluene. The mixture was washed with water and concentrated and the crude product purified by silica chromatography (5−20% ethyl acetate in isohexane) to afford **29** (0.24 g, 42%) as a pale yellow solid: ^{1}H NMR δ 1.93−2.09 (1H, m), 2.19−2.37 (1H, m), 2.54−2.80 (4H, m), 7.25−7.45 (7H, m), 7.48 (2H, d), 7.67 (1H, t), 7.77−7.88 (1H, m), 8.09 (2H, d), 8.42 (1H, s); m/z (ES+), $(M + H)^+$ = 361.

1-(4-(3-Phenylquinolin-2-yl)phenyl)cyclobutanecarboxylic Acid (30). KOH (111 mg, 2 mmol) was added to **29** (238 mg, 0.7 mmol) in 2,2′-oxidiethanol (1.9 mL) and the resulting mixture stirred at 245 °C for 75 min in a microwave reactor. The reaction mixture was allowed to cool to room temperature, diluted with water, and adjusted to pH 4.6 with aq HCl (2 M). The precipitate was collected by filtration, washed with water, and dried and the crude product purified by silica chromatography (0−100% ethyl acetate in dichloromethane) to afford **30** (135 mg, 54%) as a beige solid: ^{1}H NMR δ 1.80 (1H, dq),

1.86−2.02 (1H, m), 2.37 (2H, ddd), 2.63−2.76 (2H, m), 7.21 (2H, d), 7.26−7.43 (7H, m), 7.65 (1H, dd), 7.76−7.86 (1H, m), 8.07 (2H, d), 8.39 (1H, s), 12.32 (1H, s); *m/z* (ES+), (M + H)⁺ = 380.

2-(4-(1-Isocyanatocyclobutyl)phenyl)-3-phenylquinoline (31). DPPA (92 μL, 0.4 mmol) was added to **30** (108 mg, 0.3 mmol) and Et₃N (59 μL, 0.4 mmol) in dichloromethane (1 mL) and the mixture stirred at 25 °C for 4 h. The reaction mixture was diluted with dichloromethane and water, and the organic layer was washed with brine, dried, and concentrated to afford **31** (107 mg) which was used without further purification: *m/z* (ES+) (M + H)⁺ = 377.

1-(4-(3-Phenylquinolin-2-yl)phenyl)cyclobutanamine (3). Compound **31** (107 mg, 0.3 mmol) in aq HCl (2 M, 2.5 mL, 5 mmol) was stirred at 60 °C for 5.5 h. The reaction mixture was cooled to room temperature, diluted with methanol, and purified by ion exchange chromatography, using a 5 g SCX-3 column (7 M NH₃/methanol) to afford crude product which was further purified by silica chromatography (50−100% ethyl acetate in isohexane) to afford **3** (59 mg, 60%) as a white foamy solid: ¹H NMR δ 1.57−1.71 (1H, m), 1.93−2.12 (5H, m), 2.30−2.42 (2H, m), 7.27−7.41 (9H, m), 7.60−7.68 (1H, m), 7.80 (1H, ddd), 8.07 (2H, dd), 8.38 (1H, s); HRMS *m/z* (ES+) (M + H)⁺ = 351.185 36 (theoretical 351.185 58).

6-Chloro-5-phenylpyridazin-3-amine (33). NH₃ in methanol (7 M, 2.29 mL, 16 mmol) and **32** (1 g, 4.4 mmol) were dissolved in ethanol (14.1 mL) and heated at 150 °C for 24 h in a microwave reactor and then cooled to room temperature. The reaction mixture was evaporated, dissolved in dichloromethane (100 mL), and washed sequentially with saturated aq NaHCO₃ (50 mL) and brine (50 mL). The organic layer was dried and evaporated to afford crude product which was purified by silica chromatography (0−5% methanol in dichloromethane) to afford **33** (0.45 g, 49%) as a white solid: ¹H NMR δ 6.66 (2H, s), 6.80 (1H, s), 7.45−7.56 (5H, m); *m/z* (ES+) (M + H)⁺ = 206.

6-Chloro-7-phenylimidazo[1,2-b]pyridazine (34). Compound **33** (360 mg, 1.8 mmol) in ethanol (4 mL) was stirred at 60 °C. Aqueous 2-chloroacetaldehyde (55%, 2.0 mL, 7 mmol) was added dropwise, and the reaction mixture was stirred at 60 °C for 16 h, cooled to room temperature, diluted with ethyl acetate (30 mL), washed with saturated aq NaHCO₃ (2 × 20 mL), dried, and evaporated to give a solid. The solid was triturated with isohexane and collected by filtration to afford **34** (325 mg, 81%) as a pale yellow solid: ¹H NMR δ 7.45−7.59 (5H, m), 7.89 (1H, d), 8.21 (1H, d), 8.37−8.40 (1H, m); *m/z* (ES+) (M + H)⁺ = 230.

1-(4-(7-Phenylimidazo[1,2-b]pyridazin-6-yl)phenyl)-cyclobutanamine (5). *tert*-Butyl 1-(4-(4,4,5,5-tetramethyl-1,3,2-dioxaborolan-2-yl)phenyl)cyclobutylcarbamate (163 mg, 0.4 mmol), **34** (100 mg, 0.4 mmol), diacetoxyzinc (88 mg, 0.5 mmol), aq Na₂CO₃ (2 M, 653 μL, 1.3 mmol), and Pd(PPh₃)₄ (25 mg, 0.02 mmol) were suspended in dioxane and heated at 100 °C for 2 h in a microwave reactor and then cooled to room temperature, and the organic phase was decanted from the solidified Na₂CO₃ layer. The reaction mixture was evaporated to dryness to afford crude product which was purified by silica chromatography (0−5% methanol in dichloromethane) to afford a yellow oil. TFA (454 μL) was added to a solution of this in dichloromethane (454 μL) and the solution was stirred at room temperature for 1 h. The reaction mixture was evaporated and dissolved in methanol. The crude product was purified by ion exchange chromatography, using an SCX column (7 M NH₃/methanol) to afford crude product. The product was further purified by silica chromatography (0−10% methanol in dichloromethane) to afford **5** (37 mg, 48%) as a white crystalline solid: ¹H NMR (MeOD) δ 1.69−1.84 (1H, m), 2.02−2.15 (1H, m), 2.21−2.33 (2H, m), 2.50−2.60 (2H, m), 7.20−7.33 (5H, m), 7.33−7.43 (4H, m), 7.80 (1H, d), 7.95 (1H, d), 8.15−8.19 (1H, m), 1 × NH₂ not observed; *m/z* (ES+) (M + H)⁺ = 341.

***tert*-Butyl *N*-[1-[4-(2-Trimethylsilylethynyl)phenyl]-cyclobutyl]carbamate (36).** *tert*-Butyl 1-(4-bromophenyl)-cyclobutylcarbamate **35** (4 g, 12.3 mmol) and ethynyltrimethylsilane (4.25 mL, 30.7 mmol) were stirred in tetrahydrofuran (150 mL). Pd(PPh₃)₂Cl₂ (0.43 g, 0.6 mmol), CuI (47 mg, 0.25 mmol), and triphenylphosphine (0.32 g, 1.2 mmol) were added, followed by

triethylamine (5.13 mL, 36.8 mmol). The solution was heated at 70 °C for 18 h. Further portions of Pd(PPh₃)₂Cl₂ (0.22 g, 0.3 mmol) and CuI (23 mg, 0.12 mmol) were added followed by ethynyltrimethylsilane (2.12 mL, 15.3 mmol), and stirring was continued under nitrogen at 70 °C for 5 h, and then the mixture was allowed to cool to room temperature. The reaction mixture was filtered, concentrated, and then purified by silica chromatography (0−6% ethyl acetate in isohexane) to afford **36** (930 mg, 22%) as a yellow solid: ¹H NMR δ 0.00 (9H, s), 0.95 and 1.09 (9H, 2 × bs), 1.45−1.61 (1H, m), 1.67−1.82 (1H, m), 2.06−2.20 (4H, m), 7.15 (4H, dd), 7.38 (1H, s); *m/z* (ES−) (M − H)⁻ = 342.

***tert*-Butyl 1-(4-Ethynylphenyl)cyclobutylcarbamate (37).** Compound **36** (930 mg, 2.7 mmol) was dissolved in methanol (45 mL) and K₂CO₃ (4.62 g, 33.4 mmol) was added. The slurry was stirred at room temperature for 2.5 h and then concentrated. Water (40 mL) was added and the mixture was extracted with ethyl acetate (3 × 25 mL). The combined extracts were washed with brine, dried, and evaporated to afford **37** (0.73 g, 22%) as a brown gum which was used without further purification: ¹H NMR δ 0.90 and 1.10 (9H, 2 × bs), 1.47−1.63 (1H, m), 1.68−1.84 (1H, m), 2.06−2.23 (4H, m), 3.87 (1H, s), 7.08−7.31 (4H, m), 7.39 (1H, bs); *m/z* (ES−) (M−H)⁻ = 270.

Ethyl 3-(4-(1-(*tert*-Butoxycarbonyl(ethoxycarbonyl)amino)-cyclobutyl)phenyl)propiolate (38). LDA in tetrahydrofuran (1.8 M, 0.74 mL, 1.3 mmol) was added to **37** (100 mg, 0.4 mmol) in tetrahydrofuran (5 mL) at −78 °C. The resulting solution was stirred at −78 °C for 20 min, ethyl chloroformate (0.12 mL, 1.3 mmol) was added, and the mixture was allowed to warm to room temperature and stirred for 1 h. The reaction was diluted with ethyl acetate (10 mL) and washed with water (2 × 10 mL) and brine (10 mL). The organic layer was dried and evaporated to afford crude product which was purified by silica chromatography (0−20% ethyl acetate in isohexane) to afford **38** (99 mg, 65%) as a colorless oil: ¹H NMR (CDCl₃) δ 1.25 (3H, t), 1.36 (3H, t), 1.41 (9H, s), 1.72−1.90 (2H, m), 2.52−2.71 (4H, m), 4.18 (2H, q), 4.25−4.33 (2H, m), 7.53−7.59 (2H, m), 7.64−7.68 (2H, m). No molecular ion was observable.

Ethyl 2-(4-(1-(*tert*-Butoxycarbonyl(ethoxycarbonyl)amino)-cyclobutyl)phenyl)pyrazolo[1,5-a]pyridine-3-carboxylate (39). A solution of DBU (286 mg, 1.9 mmol) in acetonitrile (5 mL) was added dropwise to **38** (390 mg, 0.9 mmol) and 1-aminopyridinium iodide (208 mg, 0.9 mmol) in acetonitrile (20 mL) at 0 °C. The resulting mixture was stirred at 0 °C for 30 min and then at room temperature for 18 h. The reaction mixture was diluted with ethyl acetate (10 mL) and washed with water (2 × 10 mL) and brine (10 mL). The organic layer was dried and evaporated to afford crude product which was purified by silica chromatography (0−20% ethyl acetate in isohexane) to afford **39** (407 mg, 85%) as a colorless oil: ¹H NMR δ 1.16 (6H, dt), 1.33 (9H, s), 1.64−1.73 (1H, m), 1.73−1.83 (1H, m), 2.46−2.63 (4H, m), 4.06 (2H, q), 4.18 (2H, q), 7.12 (1H, td), 7.52−7.59 (1H, m), 7.62 (2H, d), 7.70 (2H, d), 8.09 (1H, d), 8.81 (1H, d); *m/z* (ES+) (M + H)⁺ = 508.

2-(4-(1-(*tert*-Butoxycarbonylamino)cyclobutyl)phenyl)-pyrazolo[1,5-a]pyridine-3-carboxylic Acid (40). Aqueous NaOH (2 M, 3.8 mL, 1 mmol) was added to **39** (45 mg, 0.1 mmol) in ethanol (2 mL). The resulting solution was stirred at 100 °C for 2 h and then cooled to room temperature. The reaction was concentrated and acidified with aq HCl (2 M) and then filtered to afford **40** (310 mg, 97%) as a white solid: ¹H NMR δ 1.36 (9H, s), 1.84 (1H, s), 1.95−2.10 (1H, m), 2.43 (4H, t), 7.15 (1H, t), 7.45 (2H, d), 7.52−7.63 (2H, m), 7.75 (2H, d), 8.16 (1H, d), 8.83 (1H, d), 12.26 (1H, s); *m/z* (ES−) (M − H)⁻ = 406.

***tert*-Butyl 1-(4-(3-Bromopyrazolo[1,5-a]pyridin-2-yl)phenyl)-cyclobutylcarbamate (41).** Compound **40** (290 mg, 0.7 mmol), Na₂CO₃ (179 mg, 2.1 mmol), and NBS (127 mg, 0.7 mmol) in dimethylformamide (2 mL) were stirred at room temperature for 1 h. The mixture was poured into water (150 mL) and the resulting solid collected by filtration and washed with water to afford **41** (288 mg, 91%) as a white solid: ¹H NMR δ 1.35 (9H, s), 1.78−1.88 (1H, m), 1.98−2.08 (1H, m), 2.44 (4H, t), 7.03 (1H, t), 7.37−7.44 (1H, m),

7.54 (2H, d), 7.62 (2H, d), 7.95 (2H, d), 8.77 (1H, d); *m/z* (ES+) (M + H)⁺ = 444.

tert-Butyl 1-(4-(3-Phenylpyrazolo[1,5-*a*]pyridin-2-yl)phenyl)-cyclobutylcarbamate (42). Phenylboronic acid (127 mg, 1 mmol), aq Na₂CO₃ (2 M, 0.52 mL, 1 mmol), **41** (230 mg, 0.5 mmol) and Pd(PPh₃)₂Cl₂ (37 mg, 0.05 mmol) were suspended in 18% dimethylformamide in 1,2-dimethoxyethane/water/ethanol (7:3:2) (2 mL), heated at 150 °C for 15 min in a microwave reactor, and then cooled to room temperature. The reaction mixture was diluted with ethyl acetate (20 mL) and washed with water (2 × 20 mL) and brine (20 mL). The organic layer was dried and concentrated and the residue purified by flash silica chromatography (55−80% acetonitrile in water +1% NH₄OH) to afford **42** (138 mg, 60%) as a white solid: ¹H NMR δ 1.06−1.41 (9H, m), 1.79 (1H, s), 1.99 (1H, s), 2.31−2.44 (4H, m), 6.97 (1H, td), 7.23−7.32 (1H, m), 7.35 (5H, d), 7.42 (2H, d), 7.47 (2H, d), 7.53−7.64 (2H, m), 8.76 (1H, d); *m/z* (ES+) (M + H)⁺ = 440.

1-(4-(3-Phenylpyrazolo[1,5-*a*]pyridin-2-yl)phenyl)-cyclobutanamine (6). A solution of TFA in dichloromethane (10%, 10 mL) was added to **42** (134 mg, 0.3 mmol), and the mixture was stirred at room temperature for 2 h and then concentrated. The crude product was purified by ion exchange chromatography, using an SCX column (7 M NH₃/methanol) to afford **6** (103 mg, 100%) as a white solid: ¹H NMR δ 1.60−1.72 (1H, m), 1.97−2.05 (1H, m), 2.06−2.15 (2H, m), 2.39 (2H, ddd), 2.72 (2H, bs), 6.97 (1H, td), 7.27 (1H, ddd), 7.36 (3H, dt), 7.41−7.48 (4H, m), 7.53 (3H, dd), 8.76 (1H, d); HRMS *m/z* (ES+) M⁺ = 340.180 57 (theoretical 340.180 82).

tert-Butyl 1-(4-(Imidazo[1,2-*a*]pyridin-2-yl)phenyl)-cyclobutylcarbamate (44). *tert*-Butyl 1-(4-(4,4,5,5-tetramethyl-1,3,2-dioxaborolan-2-yl)phenyl)cyclobutylcarbamate (284 mg, 0.8 mmol), aq Na₂CO₃ (2 M, 0.31 mL, 0.6 mmol), **43** (100 mg, 0.5 mmol), and Pd(PPh₃)₂Cl₂ (36 mg, 0.05 mmol) were suspended in 18% dimethylformamide in 1,2-dimethoxyethane/water/ethanol (7:3:2) (2.0 mL), and the mixture was heated at 150 °C for 10 min in a microwave reactor and then cooled to room temperature. The reaction mixture was diluted with ethyl acetate (20 mL) and washed with water (2 × 20 mL) and brine (20 mL). The organic layer was dried and evaporated to afford crude product which was purified by flash silica chromatography, with an elution gradient from 0 to 50% ethyl acetate in isohexane, to afford **44** (140 mg, 76%) as a white solid: ¹H NMR δ 1.32 (9H, d), 1.82 (1H, s), 1.97−2.07 (1H, m), 2.42 (4H, t), 6.89 (1H, td), 7.18−7.29 (1H, m), 7.44 (2H, d), 7.57 (2H, d), 7.91 (2H, d), 8.36 (1H, s), 8.52 (1H, d); *m/z* (ES+) (M + H)⁺ = 364.

tert-Butyl 1-(4-(3-Iodoimidazo[1,2-*a*]pyridin-2-yl)phenyl)-cyclobutylcarbamate (45). NIS (222 mg, 1 mmol) was added to **44** (342 mg, 0.9 mmol) in acetonitrile (10 mL). The resulting solution was stirred at room temperature for 1 h and then evaporated, and the residue was dissolved in ethyl acetate (25 mL) and washed with aq NaOH (10% w/v, 25 mL), water (25 mL), and brine (25 mL). The organic layer was dried and evaporated to afford **45** (460 mg, 100%) as a yellow solid: ¹H NMR δ 1.29 (9H, s), 1.82 (1H, s), 1.95−2.06 (1H, m), 2.43 (4H, t), 7.08 (1H, td), 7.31−7.41 (1H, m), 7.50 (2H, d), 7.58−7.66 (2H, m), 8.02 (2H, d), 8.42 (1H, d); *m/z* (ES+) M+ = 490.

tert-Butyl 1-(4-(3-Phenylimidazo[1,2-*a*]pyridin-2-yl)phenyl)-cyclobutylcarbamate (46). Phenylboronic acid (168 mg, 1.4 mmol), aq Na₂CO₃ (2 M, 0.7 mL, 1.4 mmol), **45** (450 mg, 0.9 mmol), and Pd(PPh₃)₂Cl₂ (65 mg, 0.1 mmol) were suspended in 18% dimethylformamide in 1,2-dimethoxyethane/water/ethanol (7:3:2) (6 mL), heated at 150 °C for 15 min in a microwave reactor, and then cooled to room temperature. The reaction mixture was diluted with ethyl acetate (20 mL) and washed with water (2 × 20 mL) and brine (20 mL). The organic layer was dried and concentrated and the crude product purified by silica chromatography (0−70% ethyl acetate in isohexane) to afford **46** (259 mg, 64%) as a white solid: ¹H NMR δ 1.31 (9H, s), 1.66−1.84 (1H, m), 1.90−2.03 (1H, m), 2.25−2.45 (4H, m), 6.88 (1H, t), 7.23−7.37 (3H, m), 7.42−7.70 (9H, m), 7.99 (1H, d); *m/z* (ES+) (M + H)⁺ = 440.

1-(4-(3-Phenylimidazo[1,2-*a*]pyridin-2-yl)phenyl)-cyclobutanamine (7). TFA in dichloromethane (10%, 5 mL) was added to **46** (85 mg, 0.2 mmol) and the solution was stirred at room

temperature for 2 h and then concentrated. The crude product was purified by ion exchange chromatography, using an SCX column (7 M NH₃/methanol) to afford **7** (64 mg, 98%) as a white solid: ¹H NMR δ 1.58−1.72 (1H, m), 1.93−2.05 (1H, m), 2.06−2.19 (2H, m), 2.34−2.45 (2H, m), 3.6 (2H, s), 6.89 (1H, td), 7.26−7.35 (1H, m), 7.38 (2H, d), 7.47−7.70 (8H, m), 7.99 (1H, d); HRMS *m/z* (ES+) (M + H)⁺ = 340.180 69 (theoretical 340.180 82).

1-(4-(5-Amino-3-chloropyrazin-2-yl)phenyl)-cyclobutylcarbamate (47). A tube was charged with 5-bromo-6-chloropyrazin-2-amine (100 mg, 0.5 mmol), *tert*-butyl 1-(4-(4,4,5,5-tetramethyl-1,3,2-dioxaborolan-2-yl)phenyl)cyclobutylcarbamate (179 mg, 0.5 mmol), and Pd(PPh₃)₄ (42 mg, 0.04 mmol) in dioxane (2 mL) and aq Na₂CO₃ (2 M, 0.48 mL, 1 mmol) and the reaction heated at 100 °C under microwave irradiation for 2 h. The reaction was filtered and evaporated and the crude product purified by silica chromatography (0−6% methanol in dichloromethane) to afford **47** (162 mg, 90%) as a yellow solid: ¹H NMR δ 1.17 and 1.35 (9H, 2 × bs), 1.82 (1H, s), 2.00 (1H, s), 2.41 (4H, s), 6.94 (2H, s), 7.43 (2H, d), 7.59 (2H, d), 7.93 (1H, s); *m/z* (ES−) (M − H)⁻ = 373.

tert-Butyl 1-(4-(5-Amino-3-phenylpyrazin-2-yl)phenyl)-cyclobutylcarbamate (48). A tube was charged with **47** (160 mg, 0.4 mmol), phenylboronic acid (57 mg, 0.5 mmol), and Pd(PPh₃)₄ (49 mg, 0.04 mmol) in dioxane (2 mL) and aq Na₂CO₃, (2 M, 0.43 mL, 0.9 mmol) and then heated at 110 °C under microwave irradiation for 50 min. The reaction mixture was allowed to cool to room temperature, filtered, and evaporated. The crude product was purified by silica chromatography (20−60% ethyl acetate in isohexane) to afford **48** (70 mg, 39%) as a white solid: ¹H NMR δ 1.16 and 1.32 (9H, 2 × bs), 1.76 (1H, bm), 1.99 (1H, bm), 2.26−2.42 (4H, m), 6.52 (2H, s), 7.16−7.35 (9H, m), 7.46 (1H, bs), 7.95 (1H, s); *m/z* (ES+) (M + H)⁺ = 417.

1-(4-(5-Phenylimidazo[1,2-*a*]pyrazin-6-yl)phenyl)-cyclobutanamine Hydrochloride (11). A mixture of **48** (75 mg, 0.2 mmol) and aq 2-chloroacetaldehyde (55%, 0.21 mL, 1.8 mmol) in dimethylformamide (2.5 mL) was heated at 70 °C for 1.5 h. The solution was allowed to cool to room temperature, diluted with ethyl acetate (25 mL), and washed with saturated aq NaHCO₃ (2 × 15 mL). The organic layer was dried, filtered, and evaporated and crude product purified by silica chromatography (0−3% methanol in dichloromethane) to afford a pale yellow glassy solid. The solid was dissolved in dichloromethane (2.5 mL), and HCl in dioxane (4M, 2 mL) was added dropwise. The solution was stirred at room temperature for 1 h and then evaporated to dryness to afford **11** (42 mg, 56%) as a pale orange solid: ¹H NMR δ 1.77−1.89 (1H, m), 2.16−2.28 (1H, m), 2.54−2.63 (4H, m, partially obscured by DMSO peak), 7.46−7.53 (4H, m), 7.58−7.66 (6H, m), 7.99 (1H, s), 8.72 (3H, bs), 9.36 (1H, s); HRMS *m/z* (ES+) (M + H)⁺ = 341.176 12 (theoretical 341.176 07).

tert-Butyl 1-(4-((3-Formylpyridin-4-yl)ethynyl)phenyl)-cyclobutylcarbamate (49). A solution of 4-bromoisonicotinaldehyde hydrobromide (157 mg, 0.6 mmol) and **37** (160 mg, 0.6 mmol) in acetonitrile (6 mL) was degassed with a stream of nitrogen. Pd(PPh₃)₄ (34 mg, 0.03 mmol), CuI (2.2 mg, 0.01 mmol), and Et₃N (0.25 mL, 1.8 mmol) were added and the mixture was stirred under nitrogen at room temperature for 4 days. The reaction mixture was filtered and evaporated to dryness. The residue was purified by silica chromatography (10−35% ethyl acetate in isohexane) to afford **49** (106 mg, 48%) as an orange solid: ¹H NMR δ 1.18 and 1.29 (9H, 2 × bs), 1.73−1.88 (1H, m), 1.94−2.09 (1H, m), 2.35−2.46 (4H, m), 7.49 (2H, d), 7.63−7.76 (4H, m), 8.84 (1H, d), 9.03 (1H, s), 10.48 (1H, s); *m/z* (ES+) (M + H)⁺ = 377.

tert-Butyl *N*-[1-[4-[2-[3-[(*E*)-Methoxyiminomethyl]pyridin-4-yl]ethynyl]phenyl]cyclobutyl]carbamate (50). To a solution of **49** (105 mg, 0.3 mmol) in dichloromethane (4 mL) was added Et₃N (0.04 mL, 0.3 mmol) followed by *O*-methylhydroxylamine hydrochloride (26 mg, 0.3 mmol). The solution was stirred overnight, diluted with dichloromethane (15 mL), and washed with water (15 mL). The aqueous phase was extracted with dichloromethane (2 × 15 mL). The combined extracts were washed with brine, dried, and evaporated to afford **50** (109 mg, 96%) as a brown gum. UPLC shows

a mixture of cis and trans oxime isomers: ^{1}H NMR δ 1.18 and 1.29 (9H, 2 × bs), 1.72−1.86 (1H, m), 1.93−2.08 (1H, m), 2.34−2.46 (4H, m), 3.99 (3H, d), 7.44−7.51 (2H, m), 7.56−7.73 (4H, m), 8.54 (1H, s), 8.58−8.67 (1H, m), 8.95 (1H, s); m/z (ES+) (M + H)$^+$ = 406.

***tert*-Butyl *N*-[1-[4-(4-Chloro-2,7-naphthyridin-3-yl)phenyl]-cyclobutyl]carbamate (51).** A solution of **50** (107 mg, 0.3 mmol) in DMA (1.5 mL) and CuCl$_2$ (71 mg, 0.5 mmol) was heated at 100 °C for 2 h. The solution was cooled to room temperature, diluted with ethyl acetate (5 mL), and quenched with water (5 mL). The mixture was filtered and extracted with ethyl acetate (2 × 5 mL), washed with brine, dried, and evaporated. The crude product was purified by silica chromatography (20−65% ethyl acetate in isohexane) to afford **51** (27 mg, 25%) as a colorless crystalline solid: ^{1}H NMR δ 1.20 and 1.36 (9H, 2 × bs), 1.78−1.92 (1H, m), 1.97−2.10 (1H, m), 2.40−2.51 (4H, m) partially obscured by DMSO peak, 7.53−7.58 (2H, m), 7.67 (1H, bs), 7.76−7.82 (2H, m), 8.12 (1H, d), 8.94 (1H, d), 9.61 (1H, d), 9.65 (1H, d); m/z (ES+) (M + H)$^+$ = 410.

***tert*-Butyl *N*-[1-[4-(4-Phenyl-2,7-naphthyridin-3-yl)phenyl]-cyclobutyl]carbamate (52).** Toluene (1.5 mL) was added to a mixture of **51** (25 mg, 0.06 mmol), phenylboronic acid (11.2 mg, 0.1 mmol), S-Phos (2.5 mg, 0.01 mmol), Pd(OAc)$_2$ (0.7 mg, 3.1 μmol), and powdered anhydrous potassium orthophosphate (26 mg, 0.1 mmol). The mixture was heated at 80 °C for 2 h. The reaction mixture was cooled to room temperature, diluted with ethyl acetate (6 mL), filtered, and concentrated. The crude product was purified by silica chromatography (0−3.5% methanol in dichloromethane) to afford **52** (26 mg, 94%) as a colorless gum: ^{1}H NMR δ 1.13 and 1.29 (9H, 2 × bs), 1.68−1.83 (1H, m), 1.90−2.03 (2H, m), 2.27−2.40 (4H, m), 7.24 (2H, d), 7.27−7.32 (2H, m), 7.32−7.37 (3H, m), 7.39−7.47 (3H, m), 7.46 (1H, s), 8.70 (1H, d), 9.62 (1H, d), 9.66 (1H, d); m/z (ES+) (M + H)$^+$ = 452.

1-(4-(4-Phenyl-2,7-naphthyridin-3-yl)phenyl)-cyclobutanamine (15). HCl in dioxane (4 M, 1 mL, 4 mmol) was added dropwise to a solution of **52** (25 mg, 0.06 mmol) in dichloromethane (1 mL), and the resulting yellow suspension was stirred at room temperature for 30 min. The mixture was evaporated to dryness to afford **15** (20 mg, 92%) as a yellow solid (hydrochloride): ^{1}H NMR δ 1.71−1.85 (1H, m), 2.11−2.24 (1H, m), 2.49−2.59 (4H, m), 7.32−7.38 (2H, m), 7.43−7.55 (8H, m), 8.74 (3H, bs), 8.75 (1H, d), 9.81 (1H, d), 9.82 (1H, d); m/z (ES+) (M + H)$^+$ = 352.

***tert*-Butyl 1-(4-(3-Chloro-5-cyanopyridin-2-yl)phenyl)-cyclobutylcarbamate (53).** A solution of 5,6-dichloropyridine-3-carbonitrile (80 mg, 0.5 mmol), *tert*-butyl 1-(4-(4,4,5,5-tetramethyl-1,3,2-dioxaborolan-2-yl)phenyl)cyclobutylcarbamate (173 mg, 0.5 mmol), and 1,1-bis(di-*tert*-butylphosphino)ferrocene palladium dichloride (30 mg, 0.05 mmol) in acetonitrile (1.5 mL) and aq K$_2$CO$_3$ (2 M, 0.46 mL, 0.9 mmol) was heated at reflux for 18 h and then allowed to cool to room temperature and filtered. The filtrate was evaporated to dryness and crude product purified by silica chromatography (0−1% methanol in dichloromethane) to afford **53** (124 mg, 70%) as a pale yellow gum; m/z (ES−) (M − tBuOH)$^−$ = 308.

6-(4-(1-Aminocyclobutyl)phenyl)-5-phenylnicotinamide (26). Toluene (1 mL) was added to a mixture of **53** (60 mg, 0.2 mmol), phenylboronic acid (29 mg, 0.2 mmol), S-Phos (3.85 mg, 9.38 μmol), Pd(OAc)$_2$ (1 mg, 4.7 μmol), and powdered anhydrous potassium orthophosphate (66 mg, 0.3 mmol). The mixture was heated at 80 °C for 2 h. The reaction mixture was allowed to cool to room temperature, diluted with ethyl acetate (4 mL), and filtered. The filtrate was evaporated and the crude product purified by silica chromatography (0−15% ethyl acetate in isohexane) to afford a white solid. The solid was dissolved in dichloromethane (1.5 mL) and methanol (1.5 mL), then HCl in dioxane (4 M, 6 mL, 24 mmol) was added, and the yellow solution was stirred for 3.5 h. The solution was evaporated to dryness, and the residue was triturated with a mixture of aq K$_2$CO$_3$ (2 M, 5 mL) and ethyl acetate (5 mL), filtered, and washed with water and ethyl acetate to afford **26** (34 mg, 63%) as a white solid: ^{1}H NMR δ 1.59−1.71 (1H, m), 1.94−2.15 (3H, m), 2.31−2.42 (2H, m), 3.09 (2H, bs), 7.24−7.40 (9H, m), 7.60 (1H, s), 8.22 (2H,

d), 9.09 (1H, d); HRMS m/z (ES+) (M + H)$^+$ = 344.175 66 (theoretical 344.175 74).

ASSOCIATED CONTENT

Ⓢ Supporting Information

Details of the full synthesis and spectroscopic characterization of all additional compounds and intermediates, in addition to all protocols for in vitro and in vivo experiments. This material is available free of charge via the Internet at http://pubs.acs.org.

AUTHOR INFORMATION

Corresponding Author

*Tel: +441625 517920. E-mail: jason.kettle@astrazeneca.com.

ABBREVIATIONS USED

PI3K, phosphoinositide 3-kinase; PDK1, 3-phosphoinositide dependent protein kinase-1; mTOR, mammalian target of rapamycin; PH, pleckstrin homology; ATP, adenosine triphosphate

REFERENCES

(1) Liu, P.; Cheng, H.; Roberts, T. M.; Zhao, J. J. Targeting the phosphoinositide 3-kinase pathway in cancer. *Nat. Rev. Drug Discovery* **2009**, *8*, 627−644.

(2) Courtney, K. D.; Ryan, B.; Engelman, J. A. The PI3K pathway as a drug target in human cancer. *J. Clin. Oncol.* **2010**, *28*, 1075−1083.

(3) Manning, B. D.; Cantley, L. C. Navigating downstream of AKT. *Cell* **2007**, *129*, 1261−1274.

(4) Bozulic, L.; Hemmings, B. A. PIKKing on PKB: Regulation of PKB activity by phosphorylation. *Curr. Opin Cell Biol.* **2009**, *21*, 256−261.

(5) Sarbassov, D. D.; Guertin, D. A.; Ali, S. M.; Sabatini, D. M. Phosphorylation and regulation of Akt/PKB by the rictor-mTOR complex. *Science* **2005**, *307*, 1098−1101.

(6) Pierce, L. R.; Komander, D.; Alessi, D. R. The nuts and bolts of AGC protein kinases. *Nat. Rev. Mol. Cell Biol.* **2010**, *11*, 9−22.

(7) Mattmann, M. E.; Stoops, S. L.; Lindsley, C. W. Inhibition of Akt with small molecules and biologics: Historical perspective and current status of the patent landscape. *Expert Opin. Ther. Pat.* **2011**, *21* (9), 1309−1338.

(8) Meuillet, E. J. Novel inhibitors of AKT: Assessment of a different approach targeting the pleckstrin homology domain. *Curr. Med. Chem.* **2011**, *18*, 2727−2742.

(9) Okuzumi, T.; Fiedler, D.; Zhang, C.; Gray, D. C.; Aizenstein, B.; Hoffman, R.; Shokat, K. M. Inhibitor hijacking of Akt activation. *Nat. Chem. Biol.* **2009**, *5*, 484−493.

(10) Hirai, H.; Sootome, H.; Nakatsuru, Y.; Miyama, K.; Taguchi, S.; Tsujioka, K.; Ueno, Y.; Hatch, H.; Majumder, P. K.; Pan, B.-S.; Kotani, H. MK-2206, an allosteric Akt inhibitor, enhances antitumor efficacy by standard chemotherapeutic agents or molecular targeted drugs in vitro and in vivo. *Mol. Cancer Ther.* **2010**, *9* (7), 1956−1967.

(11) Mitchell, I. S.; Blake, J. F.; Xu, R.; Kallan, N. C.; Xiao, D.; Spencer, K. L.; Bencsik, J. R.; Liang, J.; Safina, B.; Zhang, B.; Chabot, C.; Do, S. Preparation of cyclopenta[d]pyrimidine derivatives as Akt protein kinase inhibitors. PCT Int. Appl. WO2008006040, 2008.

(12) Pal, S. K.; Reckamp, K.; Yu, H.; Figlin, R. A. Akt inhibitors in clinical development for the treatment of cancer. *Expert Opin. Invest. Drugs* **2010**, *19* (11), 1355−1366.

(13) Johnson, P. D.; Leach, A.; Luke, R. W. A.; Matusiak, Z. S.; Morris, J. J. Preparation of pyrrolo[2,3-d]pyrimidine derivatives as protein kinase B inhibitors. WO2009047563.

(14) (a) Li, Y.; Liang, J.; Siu, T; Hu, E.; Rossi, M. A.; Barnett, S. F.; Defeo-Jones, D.; Jones, R. E.; Robinson, R. G.; Leander, K.; Huber, H. E.; Mittal, S.; Cosford, N.; Prasit, P. Allosteric inhibitors of Akt1 and Akt2: Discovery of [1,2,4]triazolo[3,4-*f*][1,6]naphthyridines with potent and balanced activity. *Bioorg. Med. Chem. Lett.* **2009**, *19* (3), 834−836. (b) Wu, Z.; Hartnett, J. C.; Neilson, L. A.; Robinson, R. G.;

Fu, S.; Barnett, S. F.; Defeo-Jones, D.; Jones, R. E.; Kral, A. M.; Huber, H. E.; Hartman, G. D.; Bilodeau, M. T. Development of pyridopyrimidines as potent Akt1/2 inhibitors. *Bioorg. Med. Chem. Lett.* **2008**, *18* (4), 1274−1279. (c) Lindsley, C. W.; Zhao, Z.; Leister, W. H.; Robinson, R. G.; Barnett, S. F.; Defeo-Jones, D.; Jones, R. E.; Hartman, G. D.; Huff, J. R.; Huber, H. E.; Duggan, M. E. Allosteric Akt (PKB) inhibitors: Discovery and SAR of isozyme selective inhibitors. *Bioorg. Med. Chem. Lett.* **2005**, *15* (3), 761−764.

(15) Wu, W.-I.; Voegtli, W. C.; Sturgis, H. L.; Dizon, F. P.; Vigers, G; Brandhuber, B. J Crystal structure of human AKT1 with an allosteric inhibitor reveals a new mode of kinase inhibition. *PLoS ONE* **2010**, *5* (9), e12913.

(16) Cai, Z.-W.; Zhang, Y.; Borzilleri, R. M.; Qian, L.; Barbosa, S.; Wei, D.; Zheng, X.; Wu, L.; Fan, J.; Shi, Z.; Wautlet, B. S.; Mortillo, S.; Jeyaseelan, R.; Kukral, D. W.; Kamath, A.; Marathe, P.; D'Arienzo, C.; Derbin, G.; Barrish, J. C.; Robl, J. A.; Hunt, J. T.; Lombardo, L. J.; Fargnoli, J.; Bhide, R. S. Discovery of brivanib alaninate ((S)-((R)-1-(4-(4-fluoro-2-methyl-1H-indol-5-yloxy)-5-methylpyrrolo[2,1-f]-][1,2,4]triazin-6-yloxy)propan-2-yl)2-aminopropanoate), a novel pro-drug of dual vascular endothelial growth factor receptor-2 and fibroblast growth factor receptor-1 kinase inhibitor (BMS-540215). *J. Med. Chem.* **2008**, *51* (6), 1976−1980.

(17) Hoelder, S.; Zuelch, A.; Baer, T.; Maier, T.; Zimmermann, A.; Beckers, T.; Gekeler, V.; Joshi, H.; Munot, Y.; Bhise, U.; Chavan, S.; Shivatare, S.; Patel, S.; Gore, V. Preparation of fused imidazoles for cancer treatment. PCT Int. Appl. WO2009021990, 2009.

(18) Zhao, Z.; Leister, W. H.; Robinson, R. G.; Barnett, S. F.; Defeo-Jones, D.; Jones, R. E.; Hartman, G. D.; Huff, J. R.; Huber, H. E.; Duggan, M. E.; Lindsley, C. W. Discovery of 2,3,5-trisubstituted pyridine derivatives as potent Akt1 and Akt2 dual inhibitors. *Bioorg. Med. Chem. Lett.* **2005**, *15* (4), 905−909.

(19) Yu, X.; Wu, J. Synthesis of functionalized isoquinolines via sequential cyclization/cross-coupling reactions. *J. Comb. Chem.* **2009**, *11* (5), 895−899.

(20) Hartnett, J. C.; Barnett, S. F.; Bilodeau, M. T.; Defeo-Jones, D.; Hartman, G. D.; Huber, H. E.; Jones, R. E.; Kral, A. M.; Robinson, R. G.; Wu, Z. Optimization of 2,3,5-trisubstituted pyridine derivatives as potent allosteric Akt1 and Akt2 inhibitors. *Bioorg. Med. Chem. Lett.* **2008**, *18* (6), 2194−2197.

(21) Maestro, version 9.2; Schrödinger, LLC: New York, 2011.

(22) Glide, version 5.7; Schrödinger, LLC: New York, 2011.

(23) Sohlenius-Sternbeck, A.-K.; Afzelius, L.; Prusis, P.; Neelissen, J.; Hoogstraate, J.; Johansson, J.; Floby, E.; Bengtsson, A.; Gissberg, O.; Sternbeck, J.; Petersson, C. Evaluation of the human prediction of clearance from hepatocyte and microsome intrinsic clearance for 52 drug compounds. *Xenobiotica* **2010**, *40*, 637−649.

(24) Ashwell, M. A.; Brassard, C.; Filikov, A.; Hill, J.; Koerner, S.; Lapierre, J.-M.; Liu, Y.; Namdev, N.; Nicewonger, R.; Palma, R.; Tandon, M.; Vensel, D.; Matsuda, A.; Iimura, S.; Yamamoto, Y. Preparation of substituted imidazopyridinyl-aminopyridine compounds as antitumor agents. PCT Int. Appl. WO2011082270, 2011.

(25) Bell, M. P.; O'Dowd, C. R.; Rountree, J. S. S.; Trevitt, G. P.; Harrison, T.; McFarland, M. M.. Preparation of furopyrimidine and furopyridine derivatives as AKT/PKB inhibitors. PCT Int. Appl. WO2011055115, 2011.

(26) Bell, M. P.; O'Dowd, C. R.; Zhang, L.; Tevitt, G. P.; Harrison, T.; Battacharyya, S.; Rountree, J. S. S.; Burkamp, F.; Price, S.; Macleod, C.; Elliott, R. L.; Smith, P.; Blench, T. J.; Dyke, H. J. Preparation of chromen-4-one, pyrano[2,3-c]pyridin-4-one, and 7H-pyrano[2,3-e]-indazol-4-one derivatives as anticancer agents. PCT Int. Appl. WO2011033265, 2011.